medicina

MDPI

Article

Spectrophotometric and Wound-Gap Responses of HaCaT Keratinocytes to Turmeric-Derived Silver Formulations In Vitro

Dana-Emanuela Pitic (Coţ) [1,†], Codruța-Eliza Ille [1,2,†], Mhd Kher Alsaeyd Ahmad [1,3,*], Cosmin Sinescu [1,4,*], Ramona-Amina Popovici [1], Ioana-Cristina Talpoş-Niculescu [1], Sergiu-David Bota [1,4] and Maria Suciu [5]

[1] Faculty of Dental Medicine, "Victor Babeş" University of Medicine and Pharmacy, Revolutiei Ave. 1989, No. 9, 300580 Timisoara, Romania; dana.pitic@umft.ro (D.-E.P.); ille.codruta@umft.ro (C.-E.I.); ramona.popovici@umft.ro (R.-A.P.); ioana.talpos-niculescu@umft.ro (I.-C.T.-N.); david.bota@umft.ro (S.-D.B.)
[2] Research Center of Digital and Advanced Technique for Endodontic, Restorative and Prosthetic Treatment (TADERP), "Victor Babeş" University of Medicine and Pharmacy, Revolutiei Ave. 1989, No. 9, 300580 Timisoara, Romania
[3] Doctoral School of Dental Medicine, "Victor Babeş" University of Medicine and Pharmacy, Revolutiei Ave. 1989, No. 9, 300580 Timisoara, Romania
[4] Research Center in Dental Medicine Using Conventional and Alternative Technologies, "Victor Babeş" University of Medicine and Pharmacy Timisoara, Revolutiei Ave. 1989 No. 9, 300580 Timisoara, Romania
[5] National Institute for R&D of Isotopic and Molecular Technologies, 67-103 Donat Street, 400293 Cluj-Napoca, Romania; suciu.maria@ubbcluj.ro
* Correspondence: mhd.alsaeyd-ahmad@umft.ro (M.K.A.A.); sinescu.cosmin@umft.ro (C.S.)
† These authors contributed equally to this work.

Abstract

Background and Objectives: Silver-containing nanomaterials have attracted increasing interest for antimicrobial applications in dentistry, although their epithelial compatibility remains a major concern. This study investigated the in vitro responses of human HaCaT keratinocytes to two previously characterized *Curcuma longa*-derived silver-containing formulations obtained using aqueous (AgCUR-H_2O NPs) and ethanolic (AgCUR-EtOH NPs) extracts. *Materials and Methods*: The MTT metabolic signal and extracellular lactate dehydrogenase (LDH) activity were assessed after exposure to 10–100 µg/mL of each formulation for 24 and 48 h. Wound-gap dynamics were evaluated using an in vitro scratch assay at 10 µg/mL over 72 h. *Results*: Both formulations were associated with markedly reduced MTT metabolic signals at all tested concentrations, with mean values ranging from 3.26% to 9.23% of the corresponding untreated controls. Despite this pronounced reduction, extracellular LDH activity remained below control levels at both exposure times. In the scratch assay, the residual wound openings at 72 h were 41.46% for AgCUR-H_2O NPs and 26.98% for untreated controls, relative to their respective initial openings, indicating numerically less closure with the aqueous formulation. Conversely, AgCUR-EtOH NPs exhibited irregular wound-gap dynamics, with a final opening of 139.21%, indicating net widening of the cell-free area. *Conclusions*: Both formulations were associated with markedly reduced MTT metabolic signals and distinct wound-gap dynamics. Because formulation-specific assay interference was not experimentally excluded, the discordant MTT and LDH findings may reflect cellular effects, analytical interference, or both. Further purification and biological validation are necessary before considering these silver-containing formulations for oral-health-oriented biomaterials.

Keywords: silver-containing formulations; *Curcuma longa*; HaCaT keratinocytes; cytotoxicity; lactate dehydrogenase; scratch assay

Check for updates

Academic Editor: Bruno Chrcanovic

Received: 21 October 2026
Revised: 22 November 2026
Accepted: 24 November 2026
Published: 27 November 2026

Copyright: © 2026 by the authors. Published by MDPI on behalf of the Lithuanian University of Health Sciences. Licensee MDPI, Basel, Switzerland. This article is an open access article distributed under the terms and conditions of the Creative Commons Attribution (CC BY) license.

1. Introduction

Silver nanoparticles (AgNPs) have attracted considerable attention in biomedical research owing to their broad-spectrum antimicrobial activity and potential incorporation into a wide range of therapeutic materials, including wound dressings, implant coatings, and dental biomaterials [1,2]. In dentistry, researchers have investigated silver-containing nanomaterials as antimicrobial components of restorative materials, endodontic formulations, prosthetic devices, and implant-associated coatings, particularly for their potential to reduce microbial colonization and biofilm formation [2,3]. Their antimicrobial effects have been associated with multiple processes, including silver ion release, oxidative stress, membrane disruption, and interactions with essential cellular proteins and nucleic acids [1,4]. Nevertheless, antimicrobial efficacy alone does not establish biological suitability. For materials intended to interact with living tissues, the potential benefits of silver-containing formulations must be carefully balanced against their effects on mammalian cell viability and tissue compatibility.

Plant-mediated synthesis provides an alternative route for preparing silver-containing nanomaterials using chemically complex extract matrices [5]. Plant constituents may have several overlapping roles: some may participate in the reduction of Ag^{+} to metallic Ag^{0}, while surface-associated molecules may contribute to particle capping and stabilization [5,6]. Extract components and their reaction products may also remain as residual organic constituents without necessarily functioning as reducing or stabilizing agents. Their retention should therefore be distinguished from demonstrated involvement in particle formation or surface stabilization. The characteristics of the final formulation depend on extract composition, precursor concentration, reaction conditions, and subsequent purification [5].

Among botanical sources, *Curcuma longa* L. has been investigated as a matrix for silver nanoparticle synthesis. Shameli et al. [6] reported the use of turmeric-powder extracts for silver nanoparticle synthesis and stabilization, while Alsammarraie et al. [7] investigated synthesis using aqueous turmeric extracts and the antibacterial activity of the resulting nanoparticles. Although plant-mediated synthesis may reduce reliance on selected synthetic reagents, botanical origin alone does not guarantee lower toxicity or greater biocompatibility of the final preparation. In the present formulations, the specific contributions of individual phytochemicals to reduction and surface stabilization were not experimentally resolved.

The biological activity of silver-containing nanomaterials is strongly influenced by particle size, surface chemistry, aggregation behavior, and the chemical species present in the exposure medium. In a comparative experimental investigation, Gliga et al. [8] demonstrated size-dependent cytotoxicity of silver nanoparticles in human lung epithelial cells, with cellular responses related to silver release and intracellular exposure. Furthermore, Loza et al. [9] showed that silver nanoparticles may undergo dissolution and chemical transformations in biological media, emphasizing the relevance of ionic silver and medium-dependent interactions when interpreting their biological effects. These observations are particularly important for plant-derived formulations, in which metallic nanoparticles may coexist with residual silver precursor and extract-associated organic constituents. Consequently, the measured biological response cannot necessarily be attributed to metallic nanoparticles alone.

Keratinocytes are essential components of the epithelial barrier and participate in tissue repair through coordinated processes involving cell survival, proliferation, migration, and restoration of epithelial continuity. The HaCaT cell line, originally characterized by Boukamp et al. [10], consists of spontaneously immortalized human epidermal keratinocytes. It was used here as an established human epithelial monolayer model for exploratory assessment of the two formulations. The present findings provide preliminary, model-specific epithelial information and require subsequent validation in oral or gingival

keratinocytes and organotypic oral mucosal models before conclusions about oral tissue compatibility can be drawn. However, the cellular effects of silver nanoparticles are highly formulation-dependent. Zanette et al. [11] reported concentration- and time-dependent antiproliferative effects of silver nanoparticles in HaCaT keratinocytes, while subsequent research demonstrated that citrate- and polyethylene glycol-coated silver nanoparticles produced different effects on keratinocyte viability, proliferation, cell-cycle regulation, and apoptosis [12]. Conversely, Liu et al. [13] described beneficial wound-repair-related responses to selected silver nanoparticle preparations in an experimental wound-healing model, highlighting the importance of formulation characteristics, cell type, and biological context. Together, these findings demonstrate that the effects of silver-containing nanomaterials on epithelial cells cannot be predicted solely from their antimicrobial activity or botanical origin.

A comprehensive evaluation of epithelial compatibility requires complementary experimental endpoints. The MTT assay provides information on cellular metabolic reducing activity, whereas extracellular lactate dehydrogenase (LDH) measurements are commonly used to assess changes associated with plasma membrane integrity. For example, curcumin–cisplatin treatment has been investigated in pancreatic cancer cells using MTT alongside morphological, nuclear, and mitochondrial membrane potential assessments [14]. Similarly, eugenol has been evaluated in HaCaT and JB6 Cl 41-5a cells using MTT, cell imaging, and LDH measurements [15]. Nevertheless, nanomaterials may interfere with conventional cytotoxicity assays through optical effects, adsorption of assay components, or alterations in enzymatic activity. Kroll et al. [16] demonstrated that nanoparticle-associated interference varies substantially according to the material and analytical method. More specifically, Oh et al. [17] reported that silver nanoparticles may compromise the reliability of LDH-based cytotoxicity measurements through protein adsorption and enzyme inactivation. In parallel, the in vitro scratch assay provides an accessible method for examining changes in the repopulation of a cell-free area over time [18]. However, wound-gap closure reflects the combined influence of cellular migration, proliferation, survival, and attachment, and should therefore be interpreted in conjunction with complementary viability measurements.

In our previous investigations, we characterized aqueous and ethanolic turmeric-powder-derived *Curcuma longa* extracts for their phytochemical composition, antioxidant and antimicrobial properties, and biological responses in HaCaT keratinocytes [19]. A subsequent study investigated the physicochemical properties, antibacterial activity, HGF-1 gingival fibroblast cytocompatibility, and acute vascular irritation potential of the silver-containing formulations using HET-CAM [20]. The previously reported XRD characterization also identified residual crystalline silver nitrate within these formulations [20]. This study examines how exposure of HaCaT keratinocytes to these complete silver-containing formulations affects the MTT metabolic signal, extracellular LDH activity, and wound-gap dynamics. This extends the previous work by adding a combined epithelial response profile and examining the interpretative limitations of discordant assay readouts. The previously published physicochemical information is explicitly attributed to reference [20] and provides context for the present biological investigation.

The aim of this exploratory study was to describe MTT assay signals and extracellular LDH assay readouts in HaCaT cultures exposed to the complete silver-containing formulations AgCUR-H_2O NPs and AgCUR-EtOH NPs for 24 and 48 h at nominal concentrations of 10–100 µg/mL, and wound-gap dynamics over 72 h at 10 µg/mL. Exposure concentrations were expressed as total dried formulation mass per milliliter of culture medium.

2. Materials and Methods

2.1. Preparation and Previous Characterization of Silver-Containing Formulations

Two silver-containing formulations synthesized using aqueous and ethanolic extracts of *Curcuma longa* L. were investigated in the present study. Our research group previously reported the preparation and phytochemical characterization of the parent extracts, described by Pitic et al. [19], as well as the synthesis, physicochemical characterization, antibacterial activity, and preliminary biocompatibility assessment of the resulting silver-containing formulations, described by Ahmad et al. [20].

Briefly, the aqueous (CUR-H_2O) and ethanolic (CUR-EtOH) extracts were prepared from commercial organic turmeric powder (S.C. Republica Bio-Curcuma S.R.L., Timișoara, Romania; lot P242149), labeled as 100% *Curcuma longa* powder [19]. Botanical identification was based on the supplier's labeling. Solvent-specific extraction involved maceration and ultrasound-assisted processing. Following concentration and lyophilization, each dried extract was reconstituted in its corresponding solvent to obtain a concentration of 10 mg/mL. Silver-containing formulations were synthesized using the previously reported plant-mediated synthesis protocol [20]. Each extract (50 mL) was heated to 60 °C under magnetic stirring at 250 rpm, followed by the addition of a freshly prepared aqueous $AgNO_3$ precursor solution (1 M; 1 mol/L) at an extract-to-precursor solution volume ratio of 2:1. The ethanolic reaction was maintained for 4 h, whereas the aqueous reaction proceeded for 3 h. The resulting preparations, designated AgCUR-EtOH NPs and AgCUR-H_2O NPs, respectively, were centrifuged at 6000 rpm for 30 min, dried at 40 °C, and manually ground into fine powders. No additional washing step was performed before drying.

The formulations had previously been characterized using ultraviolet–visible spectroscopy (UV–Vis), dynamic light scattering (DLS), zeta-potential measurements, X-ray diffraction (XRD), Fourier-transform infrared spectroscopy (FTIR), scanning transmission electron microscopy (STEM), and energy-dispersive X-ray spectroscopy (EDX). The principal physicochemical characteristics relevant to the interpretation of the present biological investigation are summarized in Table 1.

Table 1. Previously reported physicochemical characteristics of the *Curcuma longa*-derived silver-containing formulations investigated in the present study [20].

Characteristics	AgCUR-H_2O NPs	AgCUR-EtOH NPs
Plant-derived matrix	Aqueous extract	Ethanolic extract
$AgNO_3$ precursor concentration	1 M	1 M
Reaction duration	3 h	4 h
STEM particle size range	15–150 nm	15–175 nm
DLS Z-average diameter	264 nm	1742 nm
Polydispersity index (PDI)	0.416	0.500
Apparent zeta potential	−21.8 ± 0.8 mV	−20.4 ± 0.6 mV
XRD crystalline-phase profile	Residual $AgNO_3$; weaker Ag-associated reflections	Residual $AgNO_3$; weaker Ag-associated reflections

Abbreviations: STEM—scanning-transmission electron microscopy; DLS—dynamic light scattering; XRD—X-ray diffraction. DLS and zeta-potential measurements were previously performed at 30 °C using 2.5 mg/mL dispersions in distilled water for AgCUR-H_2O NPs and ethanol for AgCUR-EtOH NPs [20]. These measurements characterize the complete, unwashed dispersions under the stated solvent-specific conditions; therefore, they do not selectively characterize a purified metallic silver nanoparticle fraction. In addition, they do not establish colloidal stability or particle behavior in the cell-exposure medium.

Previously reported XRD patterns identified residual crystalline $AgNO_3$ and diffraction features compatible with metallic silver and a tentatively assigned oxidized silver phase [20]. These qualitative findings do not determine phase mass fractions. The designations AgCUR-H_2O NPs and AgCUR-EtOH NPs refer to the complete, unwashed dried formulations, rather than purified metallic silver nanoparticles.

All concentrations used in the cell-based experiments represent nominal total dried formulation mass per milliliter of culture medium. The 1 M $AgNO_3$ concentration in Table 1 refers to the synthesis precursor solution. Total elemental silver content, residual $AgNO_3$ content, and dissolved silver concentrations in culture medium were not quantified. Therefore, equal formulation mass concentrations do not establish equivalent silver exposure.

2.2. HaCaT Keratinocyte Cell Line and Culture Conditions

Immortalized human keratinocytes (HaCaT; CLS 300493, Cell Line Services, Eppelheim, Germany) were maintained in high-glucose Dulbecco's Modified Eagle's Medium (DMEM) (ATCC, American Type Culture Collection, Manassas, VA, USA) containing 4.5 g/L glucose, 4 mM L-glutamine, 3.7 g/L sodium bicarbonate, and 1.0 mM sodium pyruvate, supplemented with 10% fetal calf serum and 1% penicillin–streptomycin. Cells were cultured at 37 °C in a humidified atmosphere containing 5% CO_2 and at least 95% relative humidity. Upon reaching the exponential growth phase, cells were detached using trypsin, counted with a hemocytometer, and seeded according to the requirements of each assay. All assays used cells derived from a single thaw and working culture at passages 17–21.

The MTT, extracellular LDH, and scratch assays were performed using procedures based on our previously reported protocols [19]. The nanomaterials were first prepared for the analyses by resuspension in complete media at 1 mg/mL concentration, and then kept for 24 h in the incubator at 37 °C to equilibrate and reduce cell toxicity due to nutrient depletion (as recommended by ISO 10993-5 [21]). ISO 10993-12:2021, including its 2025 amendment [22,23], provides methodological reference frameworks for in vitro cytotoxicity testing and sample preparation, respectively. Stock dispersions of each formulation were prepared in DMEM at 500 µg/mL, expressed as total dried formulation mass, and homogenized by probe ultrasonication (30 s, 30 kHz). Working dispersions were obtained by dilution to the assay-specific final concentrations: 10–100 µg/mL for MTT and LDH measurements and 10 µg/mL for the scratch assay.

Untreated cells in the same exposure medium served as the reference control (absolute control). Ethanol at 1% and 10% and Tween 20 at 10% were included as additional comparison conditions.

2.3. Assessment of the MTT Metabolic Signal

The MTT assay was used to assess the relative MTT metabolic signal following exposure of HaCaT keratinocytes to the silver-containing formulations. Cells were seeded into 96-well plates at a density of 1×10^4 cells/well and allowed to adhere for 24 h. AgCUR-H_2O NPs and AgCUR-EtOH NPs were subsequently administered at final concentrations of 10, 25, 50, 75, and 100 µg/mL for 24 or 48 h. Control conditions were as described in Section 2.2. Each experimental condition was evaluated in eight technical replicate wells within the assay. At the end of exposure, MTT solution was added to a final concentration of 0.5 mg/mL, followed by incubation for 1.5 h at 37 °C. The resulting formazan was solubilized using propanol, and absorbance was measured at 550 nm with a reference wavelength of 630 nm using a BioTek EPOCH microplate reader (Santa Clara, CA, USA). The MTT signal was expressed as a percentage relative to the corresponding untreated control, assigned a value of 100% at each exposure time [19].

2.4. Assessment of Extracellular Lactate Dehydrogenase Activity

Culture supernatants collected after 24 and 48 h of exposure were analyzed using a coupled colorimetric LDH assay based on the previously reported procedure [19]. Before the MTT assay, 50 µL of culture supernatant was transferred from each experimental well into a separate 96-well plate. Each sample was mixed with 50 µL of lithium lactate solution, 50 µL of buffer, and 50 µL of the NAD-containing detection reagent, yielding a final reaction volume of 200 µL. The detection reagent contained NAD^+, iodonitrotetrazolium (INT), and phenazine methosulfate (PMS).

In this coupled reaction, LDH catalyzes the conversion of lactate to pyruvate with concomitant reduction of NAD^+ to NADH. PMS mediates electron transfer to INT, producing a colored formazan detected at 490 nm. Accordingly, the measurement reflects color formation in the coupled reaction rather than direct NADH absorbance. Absorbance was recorded after 5 min at 490 nm, with 630 nm as the reference wavelength, using a BioTek EPOCH microplate reader.

Apparent LDH assay activity per unit volume was estimated using the following expression:

$$LDH\ activity\left(\frac{mU}{mL}\right) = \frac{(\Delta A/min) \times V_t}{\varepsilon \times d \times V_s} \times 1000$$

where ΔA/min denotes the calculation term (A490 − A630)/5, obtained by dividing the reference-corrected endpoint absorbance recorded after 5 min by the reaction interval; V_t is the total reaction volume (0.200 mL); V_s is the volume of culture supernatant analyzed (0.050 mL); ε is the extinction coefficient adopted for the INT-based calculation (18.4 mM^{-1} cm^{-1}); and d is the optical path length used in the calculation (0.625 cm). The factor 1000 converts U/mL to mU/mL.

One enzyme unit corresponds to the conversion of 1 µmol of substrate per minute under the assay conditions. The formulation concentrations, exposure intervals, and comparison conditions were as described in Sections 2.2 and 2.3. Each experimental condition was evaluated in eight technical replicate wells within the assay. The measurement values were reported in mU/mL and not normalized to a maximum LDH release. The readouts were interpreted descriptively and were not converted into percentages of cell lysis, as such interpretation may be misleading.

2.5. In Vitro Scratch Assay and Wound-Gap Quantification

An exploratory in vitro scratch assay was used to investigate changes in wound-gap opening in HaCaT monolayers exposed to the silver-containing formulations. Cells were seeded in 12-well plates at a density of 1×10^5 cells/well and cultured for 48 h until complete confluence. A linear scratch was created using a sterile 1 mL pipette tip with an approximate diameter of 1.5 mm. Following removal of the culture medium, 0.5 mL of fresh exposure medium containing AgCUR-H_2O NPs or AgCUR-EtOH NPs at 10 µg/mL was added to each well. The 10 µg/mL condition corresponded to the lowest concentration investigated in the MTT and LDH assays and was used for an exploratory assessment of wound-gap dynamics at that exposure level. It was not validated as a non-cytotoxic or biologically compatible concentration.

Untreated cells, ethanol at 1% and 10%, and Tween 20 at 10% were included as comparison conditions. Each experimental condition was evaluated in eight distinct, independently treated wells ($n = 8$). Images were acquired at baseline (0 h) and after 24, 48, and 72 h using an AmScope 40X-640X (Ningbo, Zhejiang, China) inverted trinocular microscope equipped with a digital camera at 4× magnification. At subsequent observation times, the medium was replaced with fresh medium containing the corresponding formulation. The scratch

experiments were performed concurrently with the parent-extract experiments reported in reference [19], on separate plates using a distinct set of control wells.

Two wound-gap width measurements were obtained per well using ImageJ software, version 1.53f. These measurements were within-well subsamples, and the well was the experimental unit used for statistical comparisons. The geometric variable quantified was wound-gap width, measured as the shortest distance between opposing edges of the cell monolayer and expressed in μm. Residual wound opening was expressed relative to the corresponding baseline measurement:

$$\textit{Residual wound opening}\ (\%) = \frac{G_t}{G_0} \times 100$$

where G_t denotes the mean wound-gap width at time t, and G_0 denotes the mean wound-gap width at baseline. Values below 100% indicate net gap reduction, whereas values above 100% indicate net widening.

An additional distance-based parameter was calculated as $D = (G_0 - G_{72h})/2$, representing half of the net change in mean wound-gap width over 72 h. Values were expressed in μm, with positive values indicating gap narrowing and negative values indicating widening. The observations were interpreted descriptively as changes in wound-gap geometry and monolayer coverage. The assay cannot independently resolve the contributions of migration, proliferation, survival, attachment, and detachment.

2.6. Statistical Analysis

MTT, LDH, and D results were summarized as mean ± standard deviation (SD). Each assay comprised a single experimental run, with eight distinct wells per condition. Replication was therefore at the well level within that run (these did not constitute independent repetitions of the experiment). LDH supernatants and subsequent MTT measurements originated from the same exposure wells and were not counted as separate independent replicates. For the scratch assay, two width measurements within each well represented spatial subsamples. The well was the experimental unit for exploratory statistical comparisons.

Exploratory comparisons used two-sided Welch *t*-tests to compare each formulation–concentration condition with its time-matched untreated control. MTT tests used corrected absorbance ($A_{550} - A_{630}$), while LDH tests used calculated activity in mU/mL. Holm adjustment was applied separately to all 20 comparisons within each assay, covering two formulations, five concentrations, and two exposure times. Additional ethanol and Tween control conditions were described without inferential comparisons. Between-formulation differences, between-time differences, and factorial interactions were not tested.

For the scratch assay, normalized wound-opening trajectories and net gap-reduction percentages were presented descriptively. Repeated observations over time and within-well measurements were not treated as additional independent replicates. Exploratory comparisons were confined to the geometric parameter D at 72 h, using the reported means, SDs, and eight wells per condition. Holm adjustment covered the two formulation-versus-untreated-control comparisons.

Effect estimates were expressed as unstandardized mean differences, treatment minus control, with unadjusted 95% Welch confidence intervals. Adjusted *p*-values below 0.05 were considered statistically significant within the exploratory analysis. The tests assume independent, well-level errors and approximately normal outcomes; formal normality testing was not performed. Statistical interpretation was restricted to the available experimental series and did not establish reproducibility across independent experimental runs. The statistical analysis was performed using IBM SPSS Statistics software version 32.0.0.0 (IBM Corp., Armonk, NY, USA).

3. Results

3.1. Relative MTT Signals in HaCaT Keratinocytes Exposed to Silver-Containing Formulations

Relative MTT signals were assessed following exposure of HaCaT keratinocytes to AgCUR-H_2O NPs and AgCUR-EtOH NPs at 10, 25, 50, 75, and 100 µg/mL for 24 and 48 h. Signals were normalized to the mean of the corresponding untreated control at each exposure time, assigned a value of 100% (Figure 1).

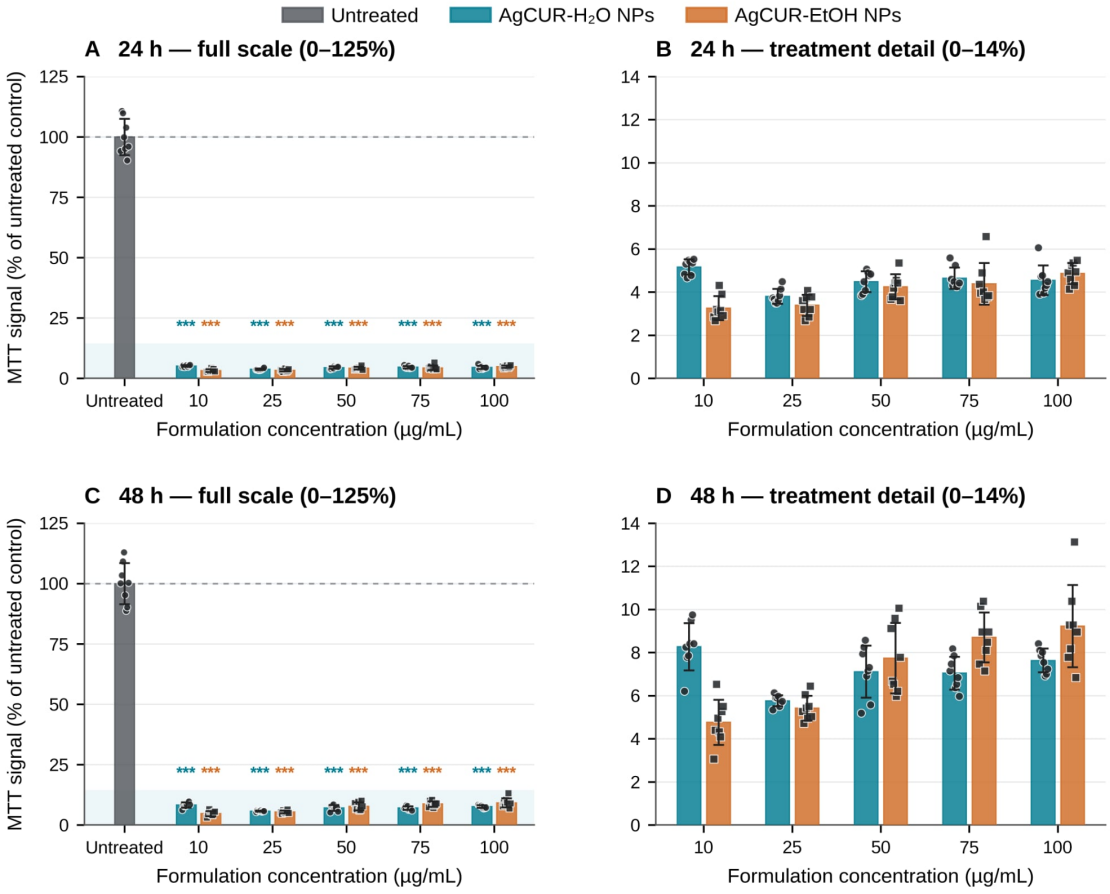


Figure 1. Relative MTT signals in HaCaT keratinocytes following exposure to *Curcuma longa*-derived silver-containing formulations for 24 h (**A**,**B**) and 48 h (**C**,**D**). Panels (**A**,**C**) show untreated controls and formulation-treated groups on the same 0–125% scale. Panels (**B**,**D**) show the same formulation-treated observations on an expanded 0–14% scale. Signals were normalized to the mean of the time-matched untreated control, assigned a value of 100%. Bars represent group means, error bars indicate SD, and overlaid points represent individual replicate wells. Each plotted group included eight technical replicate wells. Holm-adjusted *** $p < 0.001$ versus the corresponding untreated control, using two-sided Welch tests on wavelength-corrected absorbance with adjustment across 20 treatment–control comparisons. These exploratory comparisons describe variation within the available experimental series. MTT - (3-(4,5-dimethylthiazol-2-yl)-2,5-diphenyltetrazolium bromide).

After 24 h, mean relative MTT signals ranged from 3.81% to 5.17% for AgCUR-H_2O NPs and from 3.26% to 4.87% for AgCUR-EtOH NPs. After 48 h, the corresponding ranges were 5.77–8.27% and 4.77–9.23%, respectively. Mean signals therefore remained below 10% of the corresponding untreated controls throughout the investigated concentration range.

Low relative MTT signals were already recorded at 10 µg/mL, and increasing the concentration did not produce a consistent additional decline. Mean normalized signals

were numerically higher at 48 h than at 24 h for all formulation–concentration conditions. At both exposure times, all formulation-treated groups showed lower MTT signals than their corresponding untreated controls in exploratory well-level comparisons (Holm-adjusted *** $p < 0.001$).

At 24 h, formulation-treated wells and the 10% ethanol and 10% Tween 20 comparison conditions displayed low relative MTT signals. The 1% ethanol condition produced a comparatively higher MTT signal ().

3.2. Extracellular LDH Activity Following Exposure to Silver-Containing Formulations

Extracellular lactate dehydrogenase (LDH) activity was assessed in culture supernatants following exposure of HaCaT keratinocytes to AgCUR-H_2O NPs and AgCUR-EtOH NPs at 10–100 µg/mL for 24 and 48 h. Comparisons used the eight untreated-control wells from the corresponding silver-formulation experimental series at each exposure time (Figure 2).

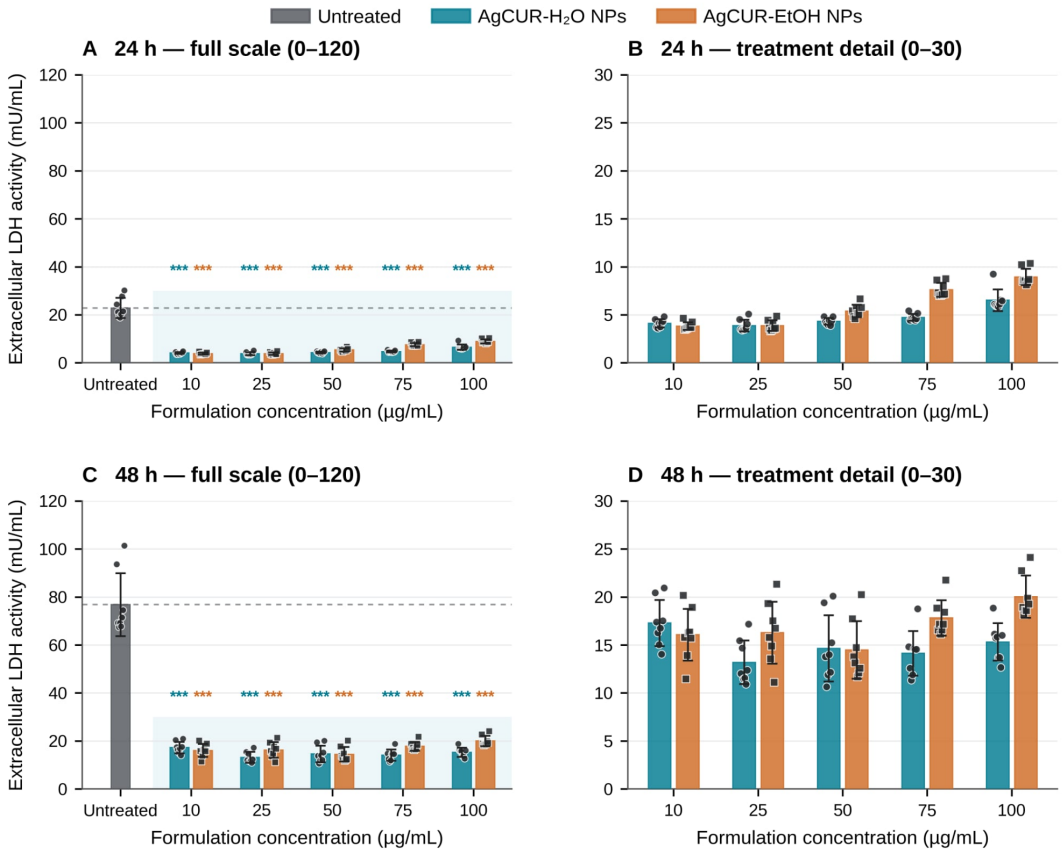


Figure 2. Extracellular LDH activity in HaCaT culture supernatants following exposure to *Curcuma longa*-derived silver-containing formulations for 24 h (**A**,**B**) and 48 h (**C**,**D**). Panels (**A**,**C**) show untreated controls and formulation-treated groups on the same 0–120 mU/mL scale. Panels (**B**,**D**) show the same formulation-treated observations on an expanded 0–30 mU/mL scale. Dashed horizontal lines indicate the corresponding untreated-control means. Bars represent group means, error bars indicate SD, and overlaid points represent individual replicate wells. Each plotted group included eight technical replicate wells within a single experimental series. Holm-adjusted *** $p < 0.001$ versus the corresponding untreated control, using two-sided Welch tests with adjustment across 20 treatment–control comparisons. These exploratory comparisons describe variation within the available experimental series. LDH - lactate dehydrogenase.

At 24 h, the untreated control showed an LDH activity of 22.90 ± 4.16 mU/mL. Mean activities ranged from 3.89 to 6.53 mU/mL for AgCUR-H_2O NPs and from 3.83 to 8.95 mU/mL for AgCUR-EtOH NPs. The mean AgCUR-EtOH NP readout increased numerically across the concentration series.

At 48 h, the untreated control showed 76.84 ± 13.12 mU/mL. Mean activities ranged from 13.21 to 17.30 mU/mL for AgCUR-H_2O NPs and from 14.50 to 20.04 mU/mL for AgCUR-EtOH NPs. Neither formulation showed a consistent monotonic concentration-related pattern at this exposure time.

Mean extracellular LDH activities were numerically higher at 48 h than at 24 h in all formulation-treated conditions. Nevertheless, all formulation-treated groups showed lower activities than their corresponding untreated controls at both exposure times in exploratory well-level comparisons (Holm-adjusted *** $p < 0.001$).

The lower calculated LDH assay activities cannot establish reduced LDH release, low cytotoxicity, or preserved membrane integrity without formulation-specific analytical validation. The concurrent low MTT signals do not independently resolve this uncertainty.

3.3. Wound-Gap Dynamics in HaCaT Keratinocyte Monolayers

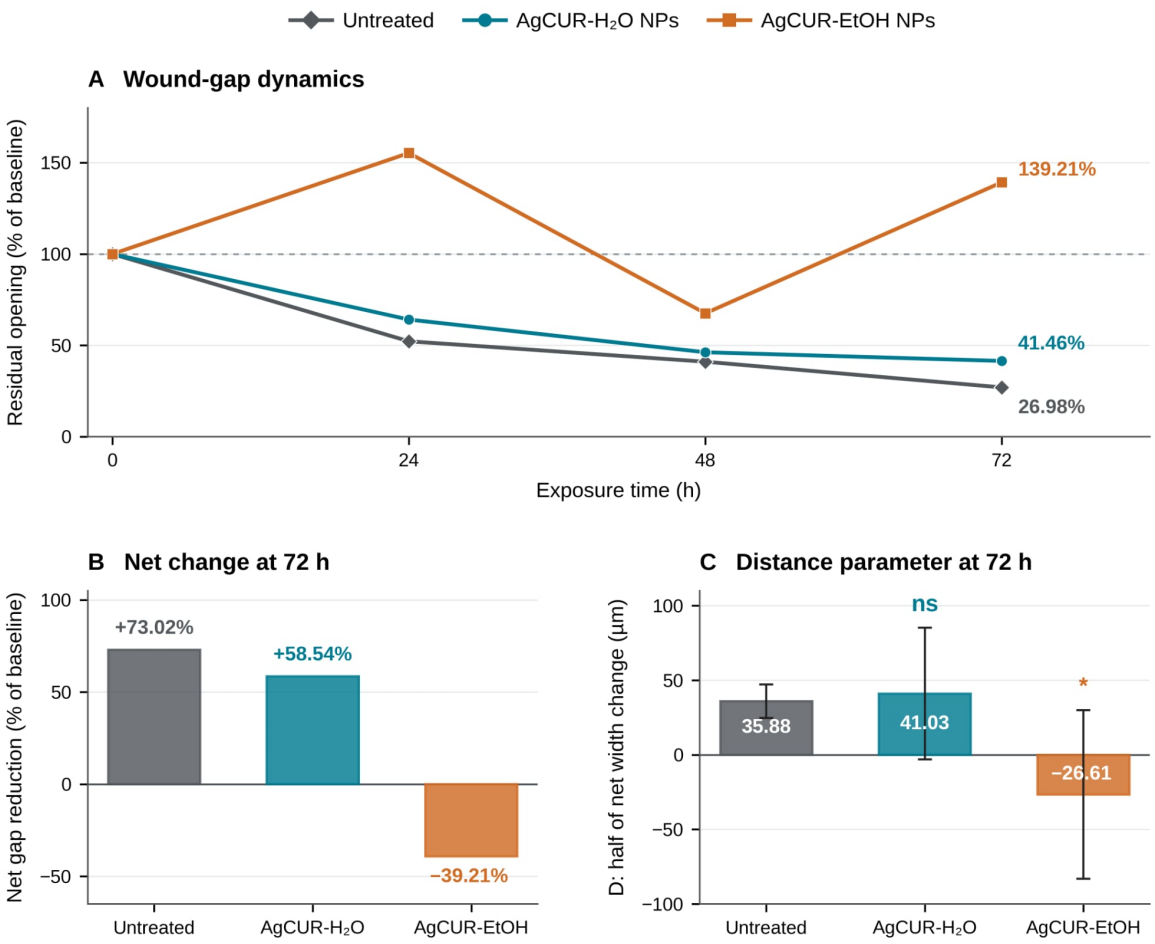
Changes in wound-gap width were evaluated in HaCaT monolayers exposed to AgCUR-H_2O NPs or AgCUR-EtOH NPs at 10 µg/mL over 72 h. Residual opening was calculated from the mean width at each observation time relative to the corresponding baseline mean (Figure 3A).

In untreated controls, residual opening decreased to 52.23%, 41.05%, and 26.98% at 24, 48, and 72 h, respectively. The corresponding values for AgCUR-H_2O NPs were 64.12%, 46.22%, and 41.46%. At 72 h, these values represented net gap reductions of 73.02% in untreated controls and 58.54% with AgCUR-H_2O NPs (Figure 3B). The aqueous formulation therefore showed numerically less normalized gap reduction than the untreated control.

AgCUR-EtOH NPs showed a non-monotonic profile, with residual openings of 155.29%, 67.53%, and 139.21% at 24, 48, and 72 h, respectively. The final value corresponded to a net widening of 39.21% relative to baseline.

The additional geometric parameter D was 35.88 ± 11.23 µm for untreated controls, 41.03 ± 44.13 µm for AgCUR-H_2O NPs, and −26.61 ± 56.49 µm for AgCUR-EtOH NPs. Exploratory comparisons using the reported means, SDs, and eight wells per condition showed no statistically significant difference between AgCUR-H_2O NPs and untreated controls (Holm-adjusted $p = 0.757$). AgCUR-EtOH NPs showed a lower D than untreated controls (Holm-adjusted $p = 0.033$). The corresponding baseline mean widths were 98.27, 140.17, and 135.72 µm for untreated controls, AgCUR-H_2O NPs, and AgCUR-EtOH NPs, respectively. D describes an absolute change in width, whereas normalized gap reduction expresses change relative to baseline. Consequently, a larger D does not necessarily indicate greater proportional gap reduction when initial widths differ.

Regarding the control conditions, exposure to 1% ethanol was associated with progressive wound-gap reduction, reaching 30.99% of the initial opening at 72 h. Conversely, 10% ethanol maintained an enlarged cell-free area throughout the observation period, with a final wound opening of 107.78%. Tween 20 (10%) was associated with a partial reduction in wound opening at 72 h, although morphological alterations were evident (Figure 4).



Formulations: 10 µg/mL. A–B: normalized summary values. C: mean ± SD; n = 8 wells/group.

C: * $p < 0.05$; ns, $p \geq 0.05$ versus untreated (Welch tests; Holm-adjusted p-values).

Figure 3. Wound-gap responses of HaCaT monolayers exposed to *Curcuma longa*-derived silver-containing formulations at 10 µg/mL. (**A**) Residual wound opening at 0, 24, 48, and 72 h, expressed relative to the corresponding baseline mean width. Markers indicate condition-level summary values. (**B**) Net gap reduction at 72 h, calculated as 100 minus residual opening; negative values indicate widening. (**C**) The geometric parameter $D = (G_0 - G_{72h})/2$, expressed as mean ± SD for eight distinct wells per condition within a single experimental run. Two width measurements were obtained within each well and were not counted as additional independent replicates. Exploratory two-sided Welch tests used the reported means, SDs, and sample sizes, with Holm adjustment for two comparisons against untreated controls. Adjusted * $p < 0.05$; ns, adjusted $p \geq 0.05$. Statistical comparisons apply only to D in panel (**C**).

Representative light microscopy images illustrate differences in HaCaT monolayer coverage and wound-edge morphology across the experimental conditions and observation times (Figure 4). In the displayed fields, cellular coverage of the scratched region was greater at 72 h than at baseline in untreated controls and AgCUR-H_2O NP-treated cultures. A visible cell-free region persisted following AgCUR-EtOH NP exposure, with irregular margins and heterogeneous cellular coverage. Ethanol (1%) panels showed relatively preserved monolayer coverage, whereas ethanol (10%) and Tween 20 (10%) panels displayed discontinuous coverage and altered cellular morphology. These images provide qualitative morphological context for the quantitative wound-gap measurements presented in Figure 3.

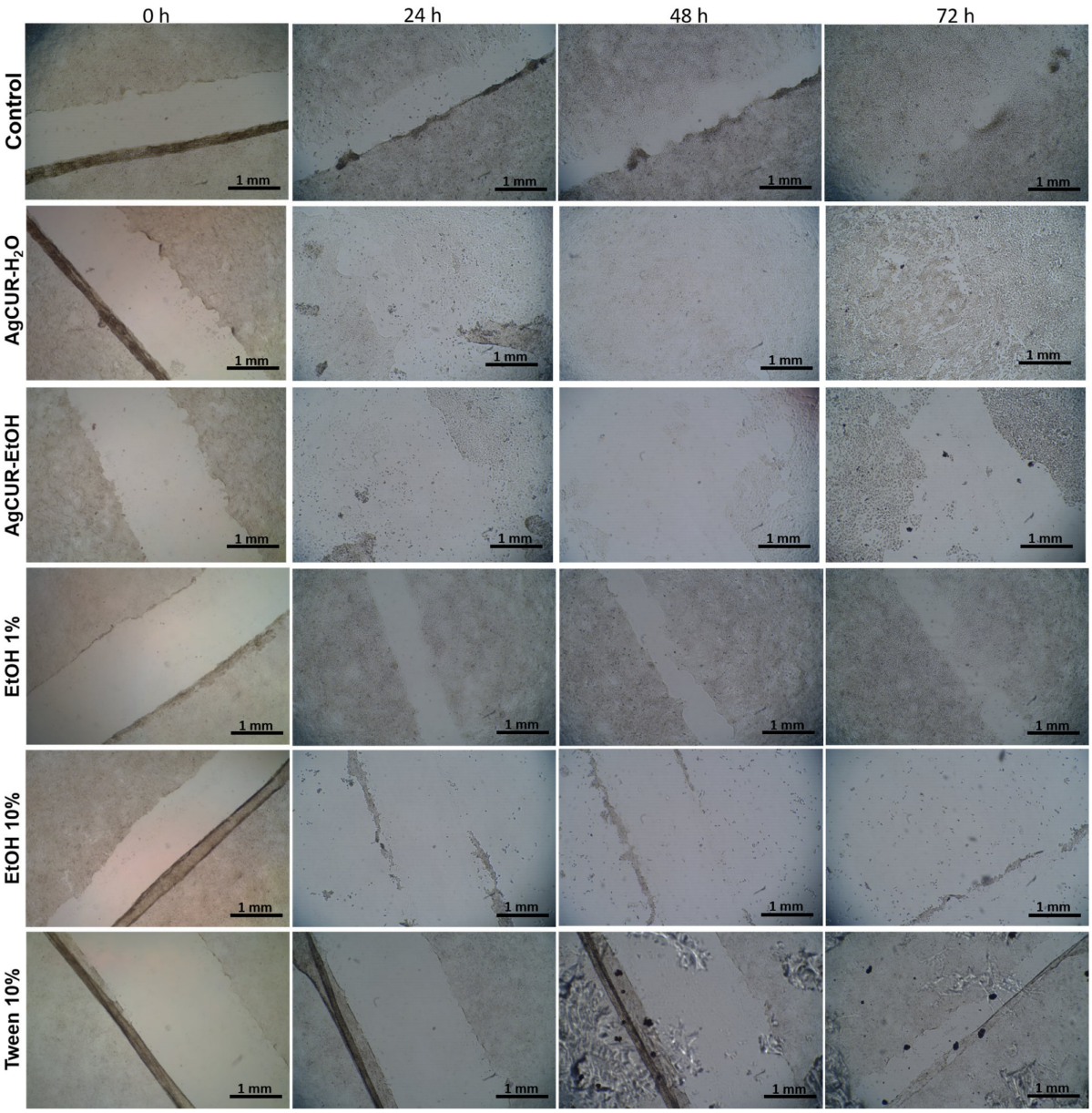


Figure 4. Representative light microscopy images of HaCaT monolayers under untreated conditions or following exposure to *Curcuma longa*-derived silver-containing formulations, AgCUR-H_2O and AgCUR-EtOH, at 10 µg/mL. Ethanol (1% and 10%) and Tween 20 (10%) were included as additional control conditions. Columns show the observation times: 0, 24, 48, and 72 h. Images for each condition follow the same well and approximately the same wound region over time. Fields were selected to illustrate representative changes in wound-edge morphology and cellular coverage. The images provide qualitative context for the quantitative wound-gap measurements presented in Figure 3. Objective magnification: 4×. Scale bars: 1 mm.

4. Discussion

The present study investigated the in vitro responses of HaCaT keratinocytes to two previously characterized *Curcuma longa*-derived silver-containing formulations, AgCUR-H_2O NPs and AgCUR-EtOH NPs, using complementary assessments of the MTT metabolic signal, extracellular lactate dehydrogenase (LDH) activity, and wound-gap dynamics. The principal findings were markedly reduced mean MTT signals at all investigated concentrations, unexpectedly reduced extracellular LDH activity relative to untreated controls, and distinct wound-gap responses between the two formulations. These observations

extend our previously published characterization and biological evaluation of the same materials [19,20] by providing additional information on their interaction with a human keratinocyte model.

4.1. Metabolic Response of HaCaT Keratinocytes to Silver-Containing Formulations

Both formulations were associated with MTT signals below 10% of untreated controls across the investigated concentration range of 10–100 µg/mL after 24 and 48 h. Low signals were already recorded at 10 µg/mL, without a consistent additional decrease at higher concentrations. Mean MTT signals were numerically higher at 48 h than at 24 h. This descriptive pattern does not establish cellular recovery, and an association between MTT and LDH readouts was not formally tested. Methodological experiments by Ghasemi et al. demonstrated that MTT readouts depend on cell density, reagent concentration, incubation time, and non-cellular optical or chemical contributions [24]. These findings support interpreting normalized MTT signals as assay readouts rather than direct percentages of surviving cells.

Previous investigations have demonstrated that silver nanoparticles may impair keratinocyte viability, proliferation, and cellular metabolism. Zanette et al. [11] reported concentration- and time-dependent antiproliferative effects of silver nanoparticles in HaCaT keratinocytes, while a separate investigation involving primary human epidermal keratinocytes demonstrated reductions in cellular viability, metabolic activity, proliferative capacity, and migration following silver nanoparticle exposure [25]. These studies provide biological context but do not establish the cause of the low MTT signals recorded in the present study. Formulation-specific analytical interference was not excluded, and differences in material preparation, exposure conditions, cellular models, and analytical methods limit direct comparison.

Importantly, the biological effects of silver nanoparticles are highly dependent on their physicochemical characteristics. A comparative investigation of citrate- and polyethylene glycol-coated silver nanoparticles showed that surface functionalization substantially influenced HaCaT viability, proliferation, cell-cycle regulation, and apoptotic responses, even when particles had comparable nominal dimensions [12]. Similarly, metabolomic investigations in HaCaT cells have emphasized the relevance of particle size, surface chemistry, ionic silver, and oxidative stress to the cellular response [26]. Differences associated with nanoparticle storage and oxidation conditions have also been reported in human keratinocytes [27]. These findings are particularly relevant to the present formulations, which were not chemically purified after synthesis. The earlier XRD characterization identified residual crystalline $AgNO_3$ but did not quantify its proportion relative to the other silver-containing phases [20]. Consequently, the assay responses recorded in HaCaT cultures cannot be attributed exclusively to metallic nanoparticles or to differences between the original aqueous and ethanolic extracts. Reactive oxygen species, apoptosis, necrosis, mitochondrial membrane potential, and DNA damage were not assessed in this study. Mechanistic explanations drawn from the cited literature therefore remain hypotheses for the present formulations.

Another relevant consideration is that the experimental concentrations were expressed as the total mass of the dried formulations rather than their elemental silver content. The actual exposure therefore involved complex silver-containing materials of incompletely quantified composition. This prevents direct comparison with investigations reporting concentrations of purified silver nanoparticles or dissolved silver ions.

4.2. Interpretation of the Extracellular LDH Assay Readouts

At 24 and 48 h, formulation-treated cultures yielded lower calculated extracellular LDH activities than the corresponding untreated controls. These values are interpreted as apparent activities derived from the coupled colorimetric assay under the tested conditions.

Oh et al. [17] demonstrated that certain silver nanoparticle preparations can reduce detectable LDH activity through protein adsorption and enzyme inactivation. These findings justify considering assay interference, but do not establish its occurrence in the present samples. Lower readouts could also reflect differences in cell number or the amount and activity of extracellular LDH; the available data do not distinguish or rank these possibilities.

Formulation-specific cell-free controls, LDH-recovery experiments, and validated maximum-release measurements were not performed. Accordingly, the lower readouts do not demonstrate reduced LDH release, less cellular injury, or preserved membrane integrity, and cannot be converted into percentages of cell lysis. Interference has also been reported for MTT measurements with silver nanoparticles [28]; the co-occurring low MTT signals do not independently validate the LDH findings because formulation-specific interference was not excluded in either assay.

4.3. Wound-Gap Dynamics and Differential Responses Between Formulations

The scratch assay provided complementary information on changes in monolayer coverage during prolonged exposure to the two formulations. At 10 μg/mL, AgCUR-H_2O NPs were associated with a progressive reduction in wound opening, reaching approximately 41.46% of the initial gap after 72 h. In contrast, AgCUR-EtOH NPs displayed a non-monotonic response, with the wound opening reaching approximately 139.21% of its initial value at the final observation time. The corresponding geometric wound-gap parameter D was positive for AgCUR-H_2O NPs (41.03 ± 44.13 μm) and negative for AgCUR-EtOH NPs (-26.61 ± 56.49 μm). These observations indicate different net wound-gap responses between the formulations, although the high variability limits the strength of quantitative comparisons.

Previous research has demonstrated that silver nanoparticles can exert different effects on keratinocytes and fibroblasts during tissue repair. Liu et al. [13] described differential cellular responses to silver nanoparticles in a murine wound-healing model, highlighting the importance of cell type and experimental context. Other investigations have demonstrated the cytotoxic potential of silver-containing preparations toward both keratinocytes and fibroblasts, with susceptibility influenced by culture conditions and cellular environment [29].

The reduction in wound opening observed with AgCUR-H_2O NPs should not be interpreted as direct evidence of enhanced keratinocyte migration or wound-healing activity. The scratch assay provides an integrated measurement influenced by cell movement, proliferation, survival, attachment, and detachment. Standard methodological descriptions emphasize the importance of consistent gap formation and controlled imaging conditions when evaluating cellular migration [18]. Furthermore, recent methodological assessments underline that conventional two-dimensional scratch models cannot reproduce the complex multicellular and extracellular matrix-dependent processes involved in physiological wound healing [30].

These considerations are particularly important in the present study because mean MTT signals remained below 10% of untreated controls at the same concentration used for the scratch assay. It should be noted that for the MTT and LDH assays, cells are placed in contact with the test materials at a confluence of about 60%. In contrast, the scratch assay starts when cells are completely confluent. The different confluence conditions may influence the assay readouts, but their contribution was not investigated separately in

this study. Consequently, the apparent wound-gap reduction observed with the aqueous formulation may reflect a complex balance of cellular persistence, movement, and changes in monolayer organization rather than a genuine pro-migratory effect. Conversely, the net widening of the cell-free area associated with AgCUR-EtOH NPs, together with irregular wound margins and reduced cellular coverage in representative micrographs, is compatible with impaired monolayer maintenance. Nevertheless, the available data do not establish the specific contributions of cell death, detachment, and inhibited migration.

4.4. Role of Residual Silver Precursor and Formulation Composition

The previous characterization identified residual crystalline $AgNO_3$ and other silver-associated diffraction features, without quantitative phase analysis [20]. The biological assays evaluated the original dried formulations without additional washing. Silver-containing materials may undergo medium-dependent dissolution and chemical transformations [9]. Pem et al. experimentally demonstrated that biological environments can influence AgNP agglomeration, dissolution, and formation of secondary particles [31]. These findings emphasize the importance of characterizing the materials in the exposure medium; however, such transformations were not measured under the present culture conditions.

The observed assay responses concern the complete formulations at nominal concentrations based on total dried formulation mass. Equal mass concentrations do not establish equivalent exposure to particulate or dissolved silver. Total silver content, residual precursor content, and dissolved silver levels were not quantified; $AgNO_3$ controls and comparisons with purified preparations were not included. Differences between the formulation profiles are therefore discussed as descriptive associations. The data do not isolate the contributions of particulate silver, residual precursor, extract-derived constituents, or their interactions, and do not establish a component-specific cause of the observed readouts. Formulation-dependent analytical effects also remain possible.

4.5. Relationship to Previously Published Biological Findings

The present results should also be considered in relation to earlier investigations of the parent *Curcuma longa* extracts and the same silver-containing formulations. In our previous study, the aqueous turmeric extract exhibited a more favorable HaCaT compatibility profile than the ethanolic extract, while both extracts supported wound-gap reduction at 10 µg/mL [19]. In the present study, both complete silver-containing formulations yielded markedly reduced relative MTT assay signals in HaCaT cultures. Comparison with the parent-extract findings provides context but does not establish a causal contribution of silver incorporation, nanoparticle formation, or residual precursor to the observed readouts.

The earlier HGF-1 study reported relative MTT-assay values of 71.88% for AgCUR-EtOH NPs and 52.14% for AgCUR-H_2O NPs at 10 µg/mL after 24 h [20]. Lower relative MTT signals were recorded in HaCaT cells at the same nominal formulation concentration and exposure duration. However, both datasets were generated in separate studies using different dispersion-preparation and assay procedures. Although both studies used MTT, incubation lasted 3 h in HGF-1 and 1.5 h in HaCaT, with absorbance measurements at 570/630 nm and 550/630 nm, respectively. Percentages were normalized to the untreated controls within each study. These methodological differences and unresolved formulation-specific assay interference in the present study prevent attribution of the contrast solely to cell type. The comparison therefore provides context but does not establish intrinsically greater sensitivity of HaCaT keratinocytes. Such an inference would require a direct comparison under standardized conditions.

HaCaT cells provide an established epidermal model for exploratory formulation assessment, but their relevance to oral applications depends on the biological endpoint con-

sidered. Han et al. directly compared HaCaT cells with telomerase-immortalized gingival keratinocytes (TIGK) and found greater migration and proliferation in TIGK, together with a different gene-expression response to injury [32]. These findings indicate that wound-gap behavior in HaCaT cultures cannot be assumed to reproduce oral epithelial repair. Complementary information can be obtained from models incorporating oral epithelial architecture and barrier function. For example, Zwicker et al. observed reduced transepithelial electrical resistance following exposure to some mouth rinses in a stratified three-dimensional buccal mucosa model, without a detectable decrease in cell viability [33]. Accordingly, the present HaCaT results provide model-specific information on formulation-associated assay signals and wound-gap dynamics. Subsequent assessment in oral or gingival keratinocytes and organotypic oral mucosal models, incorporating barrier endpoints and application-relevant exposure conditions, would be needed to evaluate oral tissue compatibility. Such investigations would address the translational relevance of the present exploratory findings.

Overall, the present study identifies markedly reduced relative MTT signals in HaCaT keratinocytes to both *Curcuma longa*-derived silver-containing formulations, accompanied by reduced detectable extracellular LDH activity and formulation-dependent changes in wound-gap dynamics. For dental biomaterial development, these findings highlight the importance of controlling residual precursor content, quantitatively characterizing silver exposure, and validating assay performance before assessing oral tissue compatibility and considering incorporation into materials intended for contact with oral tissues.

4.6. Study Limitations

Several limitations should be considered when interpreting the findings of the present study.

First, the investigated materials were unwashed silver-containing formulations with incompletely quantified composition. The previous XRD characterization identified residual crystalline $AgNO_3$ but did not establish phase mass fractions [20]. Total elemental silver, residual $AgNO_3$, and dissolved silver in the culture medium were not quantified, and $AgNO_3$ controls and comparisons with purified formulations were not included. Accordingly, the findings are limited to the tested formulations at nominal total dry-mass concentrations and cannot establish the contributions of individual silver species, extract constituents, or their interactions.

Second, exposure concentrations were expressed as nominal total dried formulation mass rather than elemental silver or purified nanoparticle concentrations, limiting comparisons with compositionally standardized materials. Across 10–100 µg/mL, MTT signals remained below 10% of untreated controls, including at the lowest concentration. The tested interval therefore did not characterize the transition from near-control MTT readouts to low signals and does not support reliable IC_{50} estimation or identification of a biologically compatible exposure range. The present dataset contains no formulation exposures below 10 µg/mL, and compatibility at lower concentrations remains undetermined. The 10 µg/mL condition used in the scratch assay corresponded to the lowest concentration in the MTT series and was not validated as a biologically compatible exposure. Further investigation of the concentration–response relationship would require formulation-specific assay validation and assessment of concentrations below 10 µg/mL.

Third, formulation-specific cell-free controls were not included in the MTT or LDH assays. Potential optical contributions, interactions with assay reagents, and changes in detectable LDH activity were therefore not experimentally excluded. Untreated cells in DMEM provided the medium control, while ethanol and Tween 20 provided additional comparison conditions; these conditions did not address formulation-specific assay interference. MTT values represent signals normalized to untreated cells and cannot be directly translated

into percentages of surviving cells. Similarly, reduced detectable extracellular LDH activity does not establish preserved membrane integrity. Additional assay-validation controls and independent viability measurements are required to determine the extent to which the observed signals reflect cellular injury. The eight-well replication reflects technical variation within the assay and does not establish reproducibility across independent experiments. Furthermore, LDH measurements were not normalized to validated maximum enzyme release, and formulation-dependent LDH recovery was not assessed. The readouts therefore cannot quantify the proportion of lysed cells or establish preserved membrane integrity.

Fourth, the scratch assay was performed at a single formulation concentration (10 µg/mL), using eight wells per condition. Multiple measurements within each image sampled local wound geometry and did not provide independent biological replication. The limited replication and variability of the reported measurements restrict interpretation to exploratory, descriptive observations and do not establish reproducibility across independent experiments. Wound-gap changes integrate migration, proliferation, survival, attachment, and detachment; these contributions were not independently quantified. Moreover, the exposure concentration was not validated as biologically compatible, and the separate MTT measurements cannot quantify cell survival or proliferation within the scratch cultures over 72 h. The results therefore describe net wound-gap dynamics without establishing a migration-specific or wound-healing effect.

Finally, the investigation was limited to immortalized HaCaT keratinocytes in a two-dimensional monolayer model. The findings provide exploratory information for formulation assessment under the tested exposure conditions and do not establish clinical safety, oral mucosal repair, therapeutic efficacy, or oral biomaterial performance. Assessment of oral tissue compatibility would require validation in oral or gingival keratinocytes and organotypic oral mucosal models, under exposure conditions relevant to the intended dental application, as part of further preclinical evaluation.

The contribution of this study is a descriptive HaCaT dataset comprising MTT and LDH assay readouts and wound-gap observations for two previously characterized silver-containing formulations. It complements the earlier physicochemical, antimicrobial, HGF-1, and HET-CAM findings [20], while the unresolved analytical and replication limitations preclude conclusions about component-specific toxicity, mechanisms, or oral tissue compatibility.

5. Conclusions

Both *Curcuma longa*-derived silver-containing formulations yielded markedly reduced relative MTT signals in HaCaT cultures at 10–100 µg/mL, with group means below 10% of the corresponding untreated controls after 24 and 48 h. Formulation-treated cultures also yielded lower apparent extracellular LDH activities than the corresponding controls. At 10 µg/mL, the scratch assay showed incomplete gap narrowing by 72 h for AgCUR-H_2O NPs and net gap widening for AgCUR-EtOH NPs.

The spectrophotometric results describe differences in assay readouts under the tested conditions. Because formulation-specific interference was not assessed, the MTT and LDH findings do not establish the extent of cellular injury or epithelial compatibility. Their co-occurrence does not establish a biological pattern of metabolic inhibition without membrane damage or demonstrate preserved membrane integrity. Likewise, the wound-gap findings do not establish a migration-specific effect or efficacy in wound repair.

The experiments assessed complete, unwashed formulations at nominal total dry-mass concentrations and did not isolate the contributions of nanoparticles, residual silver nitrate, or extract constituents. The findings therefore remain exploratory and specific to the tested HaCaT model. Assay validation, quantitative compositional characterization,

and subsequent assessment in relevant oral models would be needed before conclusions about oral tissue compatibility could be drawn.

Author Contributions: Conceptualization, D.-E.P., C.-E.I., M.K.A.A. and C.S.; methodology, D.-E.P., C.-E.I., M.K.A.A., I.-C.T.-N. and M.S.; software, R.-A.P. and S.-D.B.; validation, C.S., R.-A.P. and M.S.; formal analysis, I.-C.T.-N., S.-D.B. and M.S.; investigation, D.-E.P., C.-E.I., M.K.A.A. and M.S.; resources, C.S. and R.-A.P.; data curation, I.-C.T.-N. and S.-D.B.; writing—original draft preparation, D.-E.P., C.-E.I., M.K.A.A. and M.S.; writing—review and editing, I.-C.T.-N. and R.-A.P.; visualization, C.S. and R.-A.P.; supervision, C.S. and R.-A.P.; project administration, D.-E.P. and M.K.A.A. All authors have read and agreed to the published version of the manuscript.

Funding: This research received no external funding.

Institutional Review Board Statement: Not applicable.

Informed Consent Statement: Not applicable.

Data Availability Statement: Original microscopy images, underlying measurements, and quantification worksheets are available from the corresponding authors upon reasonable request.

Acknowledgments: The authors would like to acknowledge Victor Babeș University of Medicine and Pharmacy, Timişoara, for its support in covering the costs of publication for this research paper.

Conflicts of Interest: The authors declare no conflicts of interest.

Abbreviations

The following abbreviations are used in this manuscript:

AgNPs	Silver nanoparticles
AgCUR-EtOH NPs	Silver-containing formulation derived from the ethanolic *Curcuma longa* extract
AgCUR-H_2O NPs	Silver-containing formulation derived from the aqueous *Curcuma longa* extract
$AgNO_3$	Silver nitrate
HaCaT	Immortalized human keratinocyte cell line
DMEM	Dulbecco's Modified Eagle's Medium
FBS	Fetal bovine serum
MTT	3-[4,5-dimethylthiazol-2-yl]-2,5-diphenyl tetrazolium bromide
LDH	Lactate dehydrogenase
SD	Standard deviation

References

1. Burdușel, A.-C.; Gherasim, O.; Grumezescu, A.M.; Mogoantă, L.; Ficai, A.; Andronescu, E. Biomedical applications of silver nanoparticles: An up-to-date overview. *Nanomaterials* **2018**, *8*, 681. [CrossRef] [PubMed]
2. Bapat, R.A.; Chaubal, T.V.; Joshi, C.P.; Bapat, P.R.; Choudhury, H.; Pandey, M.; Gorain, B.; Kesharwani, P. An overview of application of silver nanoparticles for biomaterials in dentistry. *Mater. Sci. Eng. C* **2018**, *91*, 881–898. [CrossRef] [PubMed]
3. Corrêa, J.M.; Mori, M.; Sanches, H.L.; da Cruz, A.D.; Poiate, E., Jr.; Poiate, I.A.V.P. Silver nanoparticles in dental biomaterials. *Int. J. Biomater.* **2015**, *2015*, 485275. [CrossRef] [PubMed]
4. Zhang, X.-F.; Liu, Z.-G.; Shen, W.; Gurunathan, S. Silver nanoparticles: Synthesis, characterization, properties, applications, and therapeutic approaches. *Int. J. Mol. Sci.* **2016**, *17*, 1534. [CrossRef] [PubMed]
5. Ahmed, S.; Ahmad, M.; Swami, B.L.; Ikram, S. A review on plants extract mediated synthesis of silver nanoparticles for antimicrobial applications: A green expertise. *J. Adv. Res.* **2016**, *7*, 17–28. [CrossRef] [PubMed]
6. Shameli, K.; Ahmad, M.B.; Zamanian, A.; Sangpour, P.; Shabanzadeh, P.; Abdollahi, Y.; Zargar, M. Green biosynthesis of silver nanoparticles using Curcuma longa tuber powder. *Int. J. Nanomed.* **2012**, *7*, 5603–5610. [CrossRef] [PubMed]
7. Alsammarraie, F.K.; Wang, W.; Zhou, P.; Mustapha, A.; Lin, M. Green synthesis of silver nanoparticles using turmeric extracts and investigation of their antibacterial activities. *Colloids Surf. B Biointerfaces* **2018**, *171*, 398–405. [CrossRef] [PubMed]
8. Gliga, A.R.; Skoglund, S.; Odnevall Wallinder, I.; Fadeel, B.; Karlsson, H.L. Size-dependent cytotoxicity of silver nanoparticles in human lung cells: The role of cellular uptake, agglomeration and Ag release. *Part. Fibre Toxicol.* **2014**, *11*, 11. [CrossRef] [PubMed]
9. Loza, K.; Diendorf, J.; Sengstock, C.; Ruiz-Gonzalez, L.; Gonzalez-Calbet, J.M.; Vallet-Regi, M.; Köller, M.; Epple, M. The dissolution and biological effects of silver nanoparticles in biological media. *J. Mater. Chem. B* **2014**, *2*, 1634–1643. [CrossRef] [PubMed]

10. Boukamp, P.; Petrussevska, R.T.; Breitkreutz, D.; Hornung, J.; Markham, A.; Fusenig, N.E. Normal keratinization in a spontaneously immortalized aneuploid human keratinocyte cell line. *J. Cell Biol.* **1988**, *106*, 761–771. [CrossRef] [PubMed]
11. Zanette, C.; Pelin, M.; Crosera, M.; Adami, G.; Bovenzi, M.; Larese Filon, F.; Florio, C. Silver nanoparticles exert a long-lasting antiproliferative effect on human keratinocyte HaCaT cell line. *Toxicol. In Vitro* **2011**, *25*, 1053–1060. [CrossRef] [PubMed]
12. Bastos, V.; Ferreira de Oliveira, J.M.P.; Brown, D.; Johnston, H.; Malheiro, E.; Daniel-da-Silva, A.L.; Duarte, I.F.; Santos, C.; Oliveira, H. The influence of citrate or PEG coating on silver nanoparticle toxicity to a human keratinocyte cell line. *Toxicol. Lett.* **2016**, *249*, 29–41. [CrossRef] [PubMed]
13. Liu, X.; Lee, P.-Y.; Ho, C.-M.; Lui, V.C.H.; Chen, Y.; Che, C.-M.; Tam, P.K.H.; Wong, K.K.Y. Silver nanoparticles mediate differential responses in keratinocytes and fibroblasts during skin wound healing. *ChemMedChem* **2010**, *5*, 468–475. [CrossRef] [PubMed]
14. Predescu, I.-A.; Boru, C.; Smeu, A.; Coricovac, E.-D.; Hoinoiu, B.; Tănase, A.; Dehelean, C.A. Curcumin enhances cisplatin-induced cytotoxicity in PANC-1 and MIA PACA-2 pancreatic cancer cells. *Farmacia* **2026**, *74*, 78–92. [CrossRef]
15. Breban-Schwarzkopf, D.; Danila, A.-I.; Tanase, A.D.; Munteanu, K.; Haj Ali, D.; Popovici, R.; Szuhanek, C.; Rominu, M. Eugenol—A natural alternative in dentistry: An in vitro and in ovo biosafety assessment. *Farmacia* **2024**, *72*, 1011–1018. [CrossRef]
16. Kroll, A.; Pillukat, M.H.; Hahn, D.; Schnekenburger, J. Interference of engineered nanoparticles with in vitro toxicity assays. *Arch. Toxicol.* **2012**, *86*, 1123–1136. [CrossRef] [PubMed]
17. Oh, S.-J.; Kim, H.; Liu, Y.; Han, H.-K.; Kwon, K.; Chang, K.-H.; Park, K.; Kim, Y.; Shim, K.; An, S.S.A.; et al. Incompatibility of silver nanoparticles with lactate dehydrogenase leakage assay for cellular viability test is attributed to protein binding and reactive oxygen species generation. *Toxicol. Lett.* **2014**, *225*, 422–432. [CrossRef] [PubMed]
18. Liang, C.-C.; Park, A.Y.; Guan, J.-L. In vitro scratch assay: A convenient and inexpensive method for analysis of cell migration in vitro. *Nat. Protoc.* **2007**, *2*, 329–333. [CrossRef] [PubMed]
19. Pitic (Coţ), D.-E.; Kiş, A.; Stroia, C.; Talpoş-Niculescu, I.-C.; Popovici, R.-A.; Ille, C.-E.; Sallai, A.M.; Anton, A.; Moacă, E.-A.; Muntean, E.D.; et al. New insights into the antimicrobial and wound-healing properties of turmeric-powder-derived Curcuma longa extracts for oral-health-oriented applications. *Biomedicines* **2026**, *14*, 1078. [CrossRef] [PubMed]
20. Alsaeyd Ahmad, M.K.; Chioran, D.; Pitic (Coţ), D.-E.; Moacă, E.-A.; Haj Ali, D.; Predescu, I.-A.; Hegheş, A.; Talpoş-Niculescu, C.-I.; Popovici, R.-A.; Macaşoi, I.; et al. Green-synthesized Curcuma longa-derived silver nanoparticles for oral biomaterial applications: Physicochemical characterization, antibacterial activity, preliminary cytocompatibility and in ovo biocompatibility screening. *J. Funct. Biomater.* **2026**, *17*, 357. [CrossRef] [PubMed]
21. *ISO 10993-5:2009*; Biological Evaluation of Medical Devices—Part 5: Tests for In Vitro Cytotoxicity. ISO: Geneva, Switzerland, 2009.
22. *ISO 10993-12:2021*; Biological Evaluation of Medical Devices—Part 12: Sample Preparation and Reference Materials. ISO: Geneva, Switzerland, 2021.
23. *ISO 10993-12:2021/Amd 1:2025*; Biological Evaluation of Medical Devices—Part 12: Sample Preparation and Reference Materials—Amendment 1. ISO: Geneva, Switzerland, 2025.
24. Ghasemi, M.; Turnbull, T.; Sebastian, S.; Kempson, I. The MTT Assay: Utility, Limitations, Pitfalls, and Interpretation in Bulk and Single-Cell Analysis. *Int. J. Mol. Sci.* **2021**, *22*, 12827. [CrossRef] [PubMed]
25. Szmyd, R.; Goralczyk, A.G.; Skalniak, L.; Cierniak, A.; Lipert, B.; Larese Filon, F.; Crosera, M.; Borowczyk, J.; Laczna, E.; Drukala, J.; et al. Effect of silver nanoparticles on human primary keratinocytes. *Biol. Chem.* **2013**, *394*, 113–123. [CrossRef] [PubMed]
26. Carrola, J.; Bastos, V.; Jarak, I.; Oliveira-Silva, R.; Malheiro, E.; Daniel-da-Silva, A.L.; Oliveira, H.; Santos, C.; Gil, A.M.; Duarte, I.F. Metabolomics of silver nanoparticles toxicity in HaCaT cells: Structure-activity relationships and role of ionic silver and oxidative stress. *Nanotoxicology* **2016**, *10*, 1105–1117. [CrossRef] [PubMed]
27. Ahlberg, S.; Meinke, M.C.; Werner, L.; Epple, M.; Diendorf, J.; Blume-Peytavi, U.; Lademann, J.; Vogt, A.; Rancan, F. Comparison of silver nanoparticles stored under air or argon with respect to the induction of intracellular free radicals and toxic effects toward keratinocytes. *Eur. J. Pharm. Biopharm.* **2014**, *88*, 651–657. [CrossRef] [PubMed]
28. Mello, D.F.; Trevisan, R.; Rivera, N.; Geitner, N.K.; Di Giulio, R.T.; Wiesner, M.R.; Hsu-Kim, H.; Meyer, J.N. Caveats to the use of MTT, neutral red, Hoechst and resazurin to measure silver nanoparticle cytotoxicity. *Chem. Biol. Interact.* **2020**, *315*, 108868. [CrossRef] [PubMed]
29. Poon, V.K.M.; Burd, A. In vitro cytotoxity of silver: Implication for clinical wound care. *Burns* **2004**, *30*, 140–147. [CrossRef] [PubMed]
30. Molefe, P.F.; Ghasemishahrestani, Z.; Khumalo, N.P.; Bayat, A. The in vitro wound-scratch assay: Applications, technical advances, and limitations in wound healing research. *Int. Wound J.* **2026**, *23*, e70964. [CrossRef] [PubMed]
31. Pem, B.; Ćurlin, M.; Domazet Jurašin, D.; Vrček, V.; Barbir, R.; Micek, V.; Fratila, R.M.; de la Fuente, J.M.; Vinković Vrček, I. Fate and transformation of silver nanoparticles in different biological conditions. *Beilstein J. Nanotechnol.* **2021**, *12*, 665–679. [CrossRef] [PubMed]

32. Han, C.; Zhang, Y.; Yuan, H.; Keiser, S.; Leonardo, T.; Chen, L.; Wietecha, M.; DiPietro, L.A. Transcriptomic Differences Between Immortalized Oral and Skin Keratinocytes. *FASEB J.* **2025**, *39*, e70744. [CrossRef] [PubMed]
33. Zwicker, P.; Zumpe, M.; Kramer, A.; Müller, G. A 3D Model of Human Buccal Mucosa for Compatibility Testing of Mouth Rinsing Solutions. *Pharmaceutics* **2023**, *15*, 721. [CrossRef] [PubMed]

Disclaimer/Publisher's Note: The statements, opinions and data contained in all publications are solely those of the individual author(s) and contributor(s) and not of MDPI and/or the editor(s). MDPI and/or the editor(s) disclaim responsibility for any injury to people or property resulting from any ideas, methods, instructions or products referred to in the content.